Hybrid Control for Automotive Engine Management: The Cut-Off Case.

A. Balluchi† M. Di Benedetto‡ C. Pinello† C. Rossi§ and
A. Sangiovanni–Vincentelli†¶

†PARADES, Via San Pantaleo, 66, 00186 Roma, Italy,
balluchi,pinello,alberto@parades.rm.cnr.it
‡Dipartimento di Ingegneria Elettrica, Università dell'Aquila, Poggio di Roio, 67040 L'Aquila, Italy, dibenede@giannutri.caspur.it
§Magneti Marelli S.p.A., Via del Timavo, 33, 40134 Bologna, Italy,
Carlo.Rossi@bologna.marelli.it
¶Department of Electrical Engineering and Computer Science, University of California at Berkeley, CA 94720

Abstract. A novel approach to the control of an automotive engine in the cut-off region is presented. First, a hybrid model which describes the torque generation mechanism and the power-train dynamics is developed. Then, the cut-off control problem is formulated as a hybrid optimization problem, whose solution is obtained by relaxing it to the continuous domain and mapping its solution back into the hybrid domain. A formal analysis as well as simulation results demonstrate the properties and the quality of the control law.

1 Introduction

Hybrid systems have been the subject of intensive study in the past few years with particular emphasis placed on a unified representation of the problem in terms of rigorous mathematical foundations (see [5], [10], [7], [6], [3], [4]). In our opinion, it is important to address significant domains of application of hybrid control to develop further understanding of the implications of the model on the control algorithms. In the automotive industry, engine behavior is in general partitioned into regions of operation where appropriate control action are applied to yield the desired result [2]. The region of operation considered here is characterized by the driver who, by releasing the gas pedal, requests no torque to the engine. An obvious strategy to minimize gas consumption and emissions when no torque is requested is to shut fuel injection off, an operation called *cut–off*. However, cutting off fuel injection as soon as the gas pedal is released, causes a sudden torque reduction that may result in unpleasant oscillations compromising driving comfort. The open–loop control policy implemented by the industry today, consists of air and fuel input modulation, that is, throttle closure is slowed down and, when air quantity is below a threshold, fuel injection is gradually reduced to zero. As is often the case, heuristic rule–based controls need extensive tuning, yield satisfactory solutions only in a limited range of operations and are hardly optimal with respect to the emissions and fuel consumption.

In this paper, we introduce a novel, theoretically sound, closed–loop approach to cut–off control. The "plant" consists of two parts: the engine responsible for torque generation, modeled as a combination of an Extended Finite State Machine and of a Discrete Event system, and the powertrain modeled as a fourth–order linear Continuous Time system. The goal is to control the evolution of the system from an initial condition (the state of the system when the gas pedal has been released and the manifold pressure has approached its idle regime value) to cut–off, minimizing the amplitude of the undesired oscillations. The available control actions are on fuel injection and spark ignition, the inputs to the engine, occurring only once per engine cycle for each piston. The torque generated is the output of the engine and the input to the powertrain. The powertrain dynamics contain the potential oscillatory behavior to be minimized. The wheel revolution speed and the angular velocity of the crankshaft are components of its state. The timing of the torque generation mechanism is determined by the angle of the crankshaft. Consequently, the control problem is a Hybrid System Control problem, which is further complicated by the delay between the time in which the decision on the quantity of fuel to be injected is taken (at the beginning of the exhaust phase) and the time the effect of this decision takes place (during the next expansion phase).

Our approach to the hybrid problem at hand is to relax the problem to the continuous domain assuming that the torque signal can be modulated continuously over time within a given range of values. The problem so obtained is non trivial since the objective function is non differentiable. In [1] we devised a strategy that solves this problem to yield an optimal control law for the continuous domain. Then, this solution in the continuous domain was mapped back into the discrete domain. The control algorithm used sliding mode control in a region of the state space. Sliding modes yielded a control strategy that had implementation problems since it is required a fairly large number of switchings in the injection policy. In this paper we present a novel strategy which eliminates completely the sliding mode. The solution, mapped back in the hybrid domain, is demonstrated to yield a behavior that is close (within a precisely specified bound) to the behavior of the control in the continuous case. From the application of our control strategy by our industrial partner on a commercial vehicle, the proposed solution appears to be far superior than the present, heuristic approach in performance, emission control, memory and CPU occupation.

2 Problem formulation

2.1 Plant model

In this paper, we deal with 4–stroke N–cylinder gasoline engines. Our model consists of the composition of N sub–models, one per cylinder. The single cylinder sub–model $\mathcal{M}$ consists of three parts:

1. an Extended Finite State Machine (EFSM)[1] describing pistons' behavior;

[1] A deterministic Finite State Machine is a six-tuple $M = \{I, Y, \mathcal{S}, s_0, \lambda, \gamma\}$ where I is

2. a Discrete Event system (DE)[2]modeling torque generation;
3. a Continuous Time system (CT) modeling the powertrain.

Powertrain Model. The powertrain model is described by a continuous time system model developed at Magneti Marelli Engine Control Division. The model, whose parameters have been identified and validated, contains phenomena involved in powertrain oscillations that are of interest in cut–off control. Powertrain dynamics are modeled by the linear system

$$\dot{\zeta} = A^p \zeta + b^p u \tag{1}$$

$$\dot{\phi}_c = \omega_c \tag{2}$$

State $\zeta = [\alpha_e, \omega_c, \omega_p]^T$ represents the axle torsion angle, the crankshaft revolution speed, the wheel revolution speed, and ϕ_c represents the crankshaft angle. The input signal u is the torque acting on the crank. The linearized powertrain dynamics (1) is asymptotically stable since it models a passive mechanical system, and is characterized by a real dominant pole λ_1, and a pair of conjugate complex poles $\lambda \pm j\mu$, responsible for the oscillating behavior.

Piston's behavior. The behavior of each piston in the engine is abstractly represented by the Extended Finite State Machine shown in Figure 1, where $\mathcal{S} = \{H, I, C, E\}$. The four states of the EFSM are as follows.

- *Exhaust run* (H). The piston goes up, expelling combustion exhaust gases.
- *Intake run* (I). During its down–run the piston loads the air–fuel mix.
- *Compression run* (C). During its up movement the piston compresses the loaded mix.
- *Expansion run* (E). The compressed mix combustion, generated by a spark signal, produces a sudden pressure increase which pushes the piston downwards.

The transitions of the EFSM occur when a piston reaches the bottom or top dead point. The guard condition enabling the transition is expressed in terms of the piston position $\tilde{\phi}$ measured on the crankshaft, considering the offset ϕ_{co} which corresponds to the angle the crank is mounted on the shaft. The EFSM outputs the integer variable k which is incremented by one at each transition.

Torque generation. The quantity of air entering the cylinders during the intake run is controlled by a throttle valve (often directly connected to the gas pedal). The control system keeps the fuel quantity proportional to air load, so that the combustion process produces a minimum amount of waste and is maximally

the (finite) set of inputs, Y is the (finite) set of outputs, $\mathcal{S}$ is the finite set of states, s_0 is the initial state, $\lambda : \mathcal{S} \times I \to \mathcal{S}$ is the next state function, $\gamma : \mathcal{S} \times I \to Y$ is the output function. An Extended Finite State Machine is an FSM where the input and output space are not necessarily finite and can be subsets of $\mathbb{R}^n$.

[2] A DE system is intended in the sense of [8].

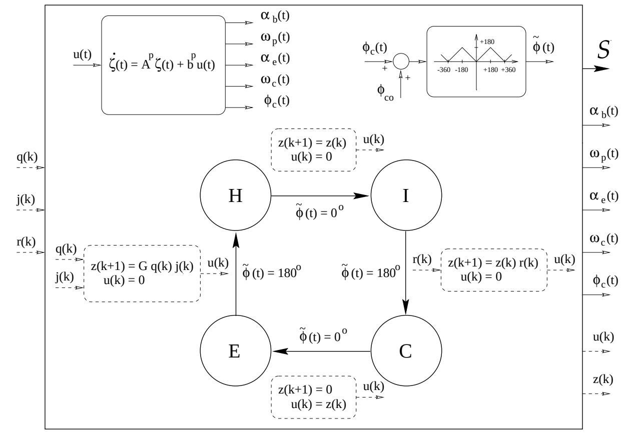

Fig. 1. Hybrid model for a single cylinder.

efficient. In electronic injection controlled engines, the fuel quantity is determined by the duration of the injection phase that takes place during the exhaust run.

The torque is generated during the expansion phase. Ideally, spark timing should occur at the precise time the piston reaches the end of its up-run in the compression phase. However, since combustion takes a non zero time to complete, it is convenient to time spark ignition before the piston concludes the compression phase. The time for spark ignition is usually refered to as *spark advance*, and it is expressed in terms of the angle the crankshaft covers before the piston reaches its next top dead center. Spark advance is not constant. It depends on temperature of the cylinders and of the loaded mix, and on the revolution speed of the crankshaft. The effect of spark advance, the other control variable considered here, is a modulation of the maximum value of torque that can be generated given the quantity and quality of the combustion mix. If the spark advance is optimal for torque generation, the modulation factor has the value 1, otherwise it is positive but less than one.

The generated torque is a complex function of time during the expansion phase, in practice it is replaced by the average value over the interval of time corresponding to the expansion phase.

The process of torque generation is characterized by the delays between the times in which fuel injection and spark advance are set and the time in which such decisions have an effect. Control signals are then subject to a transport process which can be represented by a DE system which is active at every EFSM transition. Such DE system, represented in Figure 1 with dashed boxes, receives as inputs:

- the integer k (an output of the EFSM);
- the mass of air-fuel mix $q \in \mathbb{R}^+$ loaded in the intake phase;

– a binary control variable $j \in \{0,1\}$ which indicates whether or not the fuel is present in the mix;
– the modulation factor $r \in [r_{min}, 1]$ due to non optimal spark timing.

The DE system output is the torque $u(k)$. At the EFSM transition $E \rightarrow H$ the DE system reads its inputs $q(k)$ and $j(k)$, and stores in its state $z \in \mathbb{R}$ the maximum amount of torque achievable during the next E phase, obtained by the mix-to-torque gain G. Such value is corrected at the $I \rightarrow C$ transition by the modulation factor $r(k)$ due to the chosen spark advance. The DE output $u(k)$ is always zero except at the $C \rightarrow E$ transition when it is set to the value stored in z. Between two transitions of the EFSM, occurring at times t_k and t_{k+1}, the input signal $u(t)$ to the powertrain model is given by $u(t) = u(k)$ for $t \in [t_k, t_{k+1})$.

Engine hybrid model. An engine is characterized by the number of cylinders, most cars have four, but there are engines that have a different number of cylinders[3]. The pistons are connected to the crankshaft, so that the phases of their behavior are related to each other. The overall model of torque generation for a N–cylinder engine is then the combination of N EFSMs as in Figure 1 and of N DE systems representing the behavior of each piston. The hybrid model of the complete engine is obtained by adding to torque generation model the powertrain CT dynamics (1).

In this paper we focus on the most relevant case of a 4-cylinder engine. Its model, referred to in the rest of the paper as $\mathcal{M}_{4cyl}$, has input signals $\mathbf{j} = [j_1, j_2, j_3, j_4]^T$ and $\mathbf{r} = [r_1, r_2, r_3, r_4]^T$ properly synchronized with the corresponding DE models; we denote by $\mathcal{J}_{4cyl}$ and $\mathcal{R}_{4cyl}$ the classes of functions $\mathbb{N} \rightarrow \{0,1\}^4$ and $\mathbb{N} \rightarrow [r_{min}, 1]^4$, feasible for $\mathbf{j}$ and $\mathbf{r}$. Signal q is instead shared among the cylinders. Without loss of generality, we assume that in $\mathcal{M}_{4cyl}$
- the initial EFSM states are $S_{01} = H, \;\; S_{02} = I, \;\; S_{03} = C, \;\; S_{04} = E$;
- the crankshaft offsets ϕ_{co_i} are $\phi_{co_1} = \phi_{co_3} = 180^o, \phi_{co_2} = \phi_{co_4} = 0^o$;
- the initial value of the crankshaft angle $\phi_c(0)$ is set to zero.

2.2 The optimization problem

The optimization problem is to control fuel injection and spark advance so that vehicle acceleration peaks are minimized during the cut–off operation. Throttle closure produces a decreasing evolution of the manifold pressure towards the idle regime value. We identify as the starting point of the cut–off operation the time $t_0 = t_{\bar{k}}$ at which $q_a(\bar{k})$ equals the steady-state air quantity with pedal released, q_a^o. We also assume that before t_0 the injection signals were active, so that $z_1(0) = z_2(0) = z_3(0) = z_4(0) = Gq_a^o$. To simplify notation, we set $t_0 = 0$ and $\bar{k} = 0$.

[3] For example, Formula 1 racing cars can have 8, 10 or 12 cylinders. Fiat Coupè 2000 Turbo has 5.

Assuming vehicle speed equal to wheel speed, vehicle acceleration is $a(t) = R\ \dot{\omega}_p(t)$, where R is the wheel radius. To isolate oscillations from monotone behavior, the following state transformation is applied. Set

$$\begin{bmatrix} x' \\ x \end{bmatrix} = \begin{bmatrix} P_1 \\ P_2 \end{bmatrix} \zeta = P\zeta \tag{3}$$

with $x' \in \mathbb{R}$, $x \in \mathbb{R}^2$, $P_1 \in \mathbb{R}^{1\times 3}$, and $P_2 \in \mathbb{R}^{2\times 3}$, where P is obtained from the eigenvectors of A^p. Rewrite (1) as

$$\begin{bmatrix} \dot{x}' \\ \dot{x} \end{bmatrix} = \begin{bmatrix} \lambda_1 & 0 \\ 0 & A \end{bmatrix} \begin{bmatrix} x' \\ x \end{bmatrix} + \begin{bmatrix} b' \\ b \end{bmatrix} u\ , \qquad \text{where } A = \begin{bmatrix} \lambda & -\mu \\ \mu & \lambda \end{bmatrix} . \tag{4}$$

Denoting by $c \in \mathbb{R}^{1\times 2}$ the product between the third row of A^p, the last two columns of P^{-1} and R, the oscillating component of the acceleration can be expressed as an output of the following linear system in the reduced state x

$$\dot{x}(t) = Ax(t) + bu(t) \tag{5}$$

$$\tilde{a}(t) = R\ \dot{\tilde{\omega}}_p(t) = c\ x(t)\ . \tag{6}$$

The objective of the cut–off control strategy is to minimize the peaks of the acceleration $\tilde{a}(t)$ until they are less than a threshold of perception $\tilde{a}_{th} > 0$.

Consider the circle

$$B_\rho = \left\{ x \in \mathbb{R}^2 : \|x\| \le \rho, \quad \rho = \tilde{a}_{th}\|c\|^{-1} \right\}\ , \tag{7}$$

where $\|\cdot\|$ denotes the Euclidean norm. By asymptotic stability of system (5), when $u(t) = 0$ the norm of $x(t)$ decreases over time since $\frac{d(x^T x)}{dt} = 2\lambda\, x^T x$ and $\lambda < 0$. Therefore, if at some time $\bar{t}$, the state has been driven to $x(\bar{t}) \in B_\rho$, the control $u(t) = 0$ keeps the trajectory in B_ρ and the acceleration $\tilde{a}(t)$ is bounded above by the acceleration $\tilde{a}_{th}$ for $t \ge \bar{t}$. Cut–off control problem can then be formulated as the optimization problem of steering the state x to the circle B_ρ minimizing the acceleration peak. Once in B_ρ, fuel injection can be safely shut off with vehicle oscillations below threshold.

Then the cut–off optimization problem can be formulated as follows.

Problem 1. Given the engine hybrid model $\mathcal{M}_{4cyl}$, find $\hat{\mathbf{j}} \in \mathcal{J}_{4cyl}$ and $\hat{\mathbf{r}} \in \mathcal{R}_{4cyl}$ such that

$$\sup_{0\le t\le T} |\tilde{a}(t)| \Bigg|_{\substack{\mathbf{j} = \hat{\mathbf{j}} \\ \mathbf{r} = \hat{\mathbf{r}}}} = \min_{\substack{\mathbf{j} \in \mathcal{J}_{4cyl} \\ \mathbf{r} \in \mathcal{R}_{4cyl}}} \sup_{0\le t\le T} |\tilde{a}(t)| \tag{8}$$

$$\text{subject to:} \begin{cases} \textit{Dynamics of Hybrid Model } \mathcal{M}_{4cyl} \textit{ with } \zeta(0) = \zeta_0 \textit{ s.t.} \\ x(0) = x_0 \notin B_\rho, \\ x(T) \in B_\rho, \\ z_1(0) = z_2(0) = z_3(0) = z_4(0) = Gq_a^o, \\ q(k) = q_a^o, \ \textit{for all } k \ge 0 \end{cases} \tag{9}$$

where $x_0 = P_2\zeta_0$, $x(T) = P_2\zeta(T)$, $\tilde{a}$ is given by (6), the final time T is free, $(\zeta_0, 0)^T$ is the continuous state value at the beginning of the cut-off operation, B_ρ is as in (7) and q_a^o is the steady-state air quantity with gas pedal released.

3 Continuous-time model solution

The main difficulties in Problem 1 are that the plant to be controlled is hybrid and that the input signals are bounded. Our strategy is to relax first the hybrid problem into the continuous domain, and then to map the solution back to the hybrid domain. The relaxed problem is as follows:

Problem 2. Given

$$\mathcal{U} = \{u : [0,+\infty) \to \mathbb{R} \mid u(t) \text{ is measurable and } 0 \le u(t) \le M,\ \forall t \ge 0\} \quad (10)$$

with $M = Gq_a^o$ and q_a^o the steady-state air quantity after pedal release,

$$\min_{u \in \mathcal{U}} \sup_{0 \le t \le T} |\tilde{a}(t)| \quad (11)$$

$$\text{subject to: } \begin{cases} \dot{x}(t) = Ax(t) + bu(t) \\ x(0) = x_0 \notin B_\rho \\ \|x(T)\| = \rho \end{cases} \quad (12)$$

where $|\tilde{a}(\cdot)|$ is as in (6) and T is finite.

Let $R(\theta) \in \mathbb{R}^2$ be the θ rotation matrix in $\mathbb{R}^2$ and let $(\cdot)_\perp$ be the $+\pi/2$ rotation operator defined as $z_\perp = R(\frac{\pi}{2})z$ for any $z \in \mathbb{R}^2$. Let $x_M = -A^{-1}bM$ be the equilibrium point with $u = M$ and $v = -\|x_M\|^{-1}(x_M)_\perp$. In our previous paper [1], it was shown that there exists $u \in \mathcal{U}$, which steers the state of (5) to the origin along a straight line, provided that x_0 is inside the domain $\mathcal{D}_M = \mathcal{C}_M/\mathcal{A}_v$, where $\mathcal{A}_v = \left\{x \in \mathbb{R}^2 \mid (v^T x)(b^T R(-\frac{\pi}{2})x) > 0\right\}$ and $\mathcal{C}_M = \left\{x \in \mathbb{R}^2 \mid\ x^T R(-\frac{\pi}{2})(Ax + bM) \le 0\right\}$ (see[4] Figure 2). During such motion the cost function $|\tilde{a}(\cdot)|$ monotonically decreases to zero. However, the time to reach B_ρ becomes unbounded when x_0 is such that $v^T x_0 \to 0^-$.

Proposition 3. *Let $\tilde{A} = \inf_{u \in \mathcal{U}} \sup_{0 \le t \le T} |\tilde{a}(t)|$ subject to (5). Consider*

$$\bar{u} = \begin{cases} \begin{cases} 0 & \text{if } v^T x \ge 0 \\ M & \text{if } v^T x < 0 \end{cases} & \text{if } x \notin \mathcal{D}_M \\ \begin{cases} -\frac{x^T R(-\frac{\pi}{2})Ax}{x^T R(-\frac{\pi}{2})b} & \text{if } (R(\theta)v)^T x \ge 0 \\ 0 & \text{if } (R(\theta)v)^T x < 0 \end{cases} & \text{if } x \in \mathcal{D}_M \end{cases} . \quad (13)$$

If $(cx_M)(cb) > 0$ then (13), with $\theta \in (0, \cos^{-1}(|b^T v|\,\|b\|^{-1}))$ is an optimal solution to Problem 2, i.e. $\tilde{A} = \sup_{0 \le t \le T} |\tilde{a}(t)|$ with u as in (13). Otherwise, no optimal solution in finite time exist, but, for any $\epsilon > 0$ exists $\theta > 0$ such that control (13) steers x_0 to B_ρ in finite time with $\sup_{0 \le t \le T} |\tilde{a}(t)| - \tilde{A} < \epsilon$.

For all models of existing cars available to us, $(cx_M)(cb) > 0$ was verified so (13) was actually optimal. Figure 2 reports the closed loop phase space under control (13) with $(cx_M)(cb) > 0$ and $\theta = 0$. Let $\psi(u, x_0, t)$ denote a trajectory of (5)

[4] $\mathcal{C}_M$ has center in $\frac{M}{2\mu}R(\frac{\pi}{2})b$ and radius $\frac{M}{2\mu}\|b\|$. Its boundary contains the origin (with tangent collinear to vector b) and $x_M = -A^{-1}bM$, the equilibrium point with $u = M$.

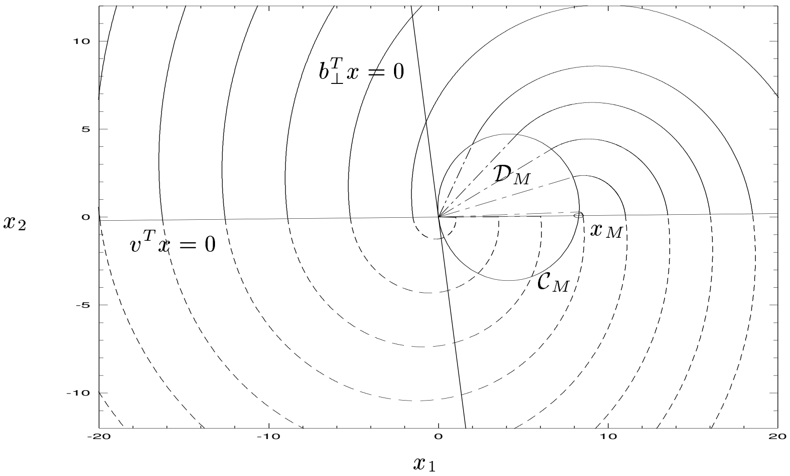

Fig. 2. Optimal trajectories for the relaxed control problem. If $x \notin \mathcal{D}_M$, u is equal to either M (continuous line) or 0 (dotted line). Otherwise $0 < u < M$ (dash-dot line).

and let $\mathcal{R}(\tau, x_0) = \{z \in \mathbb{R}^2 | \exists u \in \mathcal{U},\ \text{s.t. } z = \psi(u, x_0, \tau)\}$ be the reachable set in a specified time τ from an initial point x_0. We shall prove Proposition 3 analyzing the properties of $\mathcal{R}(\tau, x_0)$. Direct application of basic elements of trajectory analysis gives the following results.

Proposition 4. *(Proposition 5.1.1 in [9]). Given system (5) with $x(0) = x_0$ and $u \in \mathcal{U}$, the reachable set $\mathcal{R}(\tau, x_0)$ is convex and compact.*

Proposition 5. *(Theorem 8.1.1 in [9]). Given system (5) with $x(0) = x_0$ and $u \in \mathcal{U}$, if $x \in \mathcal{R}(\tau, x_0)$ then x can be reached from x_0 in time τ by means of a trajectory that corresponds to a bang–bang control with a finite number of switchings, that is $u(t) \in \{0, M\}$ for any $t \in [0, \tau]$ and $u(t)$ has finite number of discontinuity points in $[0, \tau]$.*

Proposition 6. *(Corollary 2.4.3 in [9]). Let $\psi(u, x_0, t)$ be a trajectory of (5) that corresponds to the feasible input $\hat{u}(\cdot) \in \mathcal{U}$, from x_0 to $x_\tau = \psi(u, x_0, \tau)$. Suppose that x_τ is not an interior point of $\mathcal{R}(\tau, x_0)$. Introduce the adjoint variables $p \in \mathbb{R}^2$ and Hamiltonian $H(\psi, p, \hat{u}) = p^T(Ax + b\hat{u})$. Then, there exists a trajectory $p(\cdot)$ such that $\dot{p} = -\frac{\partial H}{\partial x} = -A^T p$ with $p(t) \neq 0$ for all $t \in [0, \tau]$ and*

$$\min_{u \in \mathcal{U}} H(\psi(u, x_0, t), p(t), u(t)) = H(\psi(\hat{u}, x_0, t), p(t), \hat{u}(t)) = \nu \tag{14}$$

for almost all $t \in [0, \tau]$ with ν a constant.

Corollary 7. *Let $\psi(\hat{u}, x_0, t), p(t), \hat{u}(t)$ satisfy the minimum condition (14), then $\hat{u}(t) = M$, if $b^T p(t) > 0$, and $\hat{u}(t) = 0$, if $b^T p(t) < 0$. For any time interval of length less than or equal to $\frac{\pi}{\mu}$, $\hat{u}(t)$ has at most one discontinuity point.*

Proposition 8. *Let $\psi(\bar{u}, x_0, t)$ be the solution of (5), from x_0, with $\bar{u}$ as in (13).* (**1**) *If $\tau > 0$ is a point of local maximum for $|\tilde{a}(t)|$ and $\bar{u}(t)$ is continuous at $t = \tau$, then $\bar{u}(\tau) \in \{0, M\}$ and $x_\tau = \psi(\bar{u}, x_0, \tau)$ is such that $cA\left(x_\tau - x_M \frac{\bar{u}(\tau)}{M}\right) = 0$.*
(**2**) *If $\tau_1, \tau_2 > 0$ are two successive local maxima for $|\tilde{a}(t)|$, then $\tau_2 - \tau_1 \leq \pi/\mu$ (where equality holds if $\bar{u}(t)$ is continuous at τ_1 and τ_2), and $|\tilde{a}(\tau_1)| > |\tilde{a}(\tau_2)|$.*

Using Proposition 8, we can concentrate only on reachable sets in time $\tau \leq \frac{\pi}{\mu}$ to prove optimality of (13).

Corollary 9. *Given system (5) and input class $\mathcal{U}$, points on the boundary of the reachable set $\mathcal{R}(\tau, x_0)$, with $\tau \leq \frac{\pi}{\mu}$, are reached from x_0 by means of a bang–bang control $u : [0, \tau] \to \{0, M\}$ with at most one switching.*

The boundary of the reachable set $\mathcal{R}(\tau, x_0)$ for $\tau \leq \frac{\pi}{\mu}$, is readily obtained as

$$\partial\mathcal{R}(\tau, x_0) = \left\{x \in \mathbb{R}^2 \,|x = \gamma_0(\alpha) \vee x = \gamma_M(\alpha), \text{ with } \alpha \in [0, \tau]\right\},$$

where $\gamma_0(\cdot), \gamma_M(\cdot)$ are the parametric curves

$$\gamma_0(\alpha) = e^{A\tau}x_0 + \left(I - e^{A(\tau-\alpha)}\right)x_M, \;\; \gamma_M(\alpha) = e^{A\tau}x_0 + \left(e^{A(\tau-\alpha)} - e^{A\tau}\right)x_M$$

corresponding to $u(t) = 0$ ($u(t) = M$,resp.) for $t \in [0, \alpha)$ and $u(t) = M$ ($u(t) = 0$, resp.) for $t \in [\alpha, \tau]$. Curves $\gamma_0(\cdot), \gamma_M(\cdot)$ are of class C^∞ and $\partial\mathcal{R}(\tau, x_0)$ is closed for $\gamma_0(\tau) = \gamma_M(0) = e^{A\tau}x_0 = x^{(0)}$ and $\gamma_M(\tau) = \gamma_0(0) = e^{A\tau}(x_0 - x_M) + x_M = x^{(M)}$. However, curve $\partial\mathcal{R}(\tau, x_0)$ is not, in general, of class C^1 at $x^{(0)}$ and $x^{(M)}$, since

$$\frac{\partial\gamma_0}{\partial\alpha} = Ae^{A(\tau-\alpha)}x_M \text{ and } \frac{\partial\gamma_M}{\partial\alpha} = -Ae^{A(\tau-\alpha)}x_M \;. \tag{15}$$

Proof of Proposition 3. We shall first consider the case $\theta = 0$ in (13) and discuss later the introduction of a $\theta \neq 0$. Let $\psi(\bar{u}, x_0, t)$ be a trajectory of system (5) corresponding to control $\bar{u}$ as in (13), with $\theta = 0$, from an intial condition x_0. Note that, for any t such that $\psi(\bar{u}, x_0, t) \notin \mathcal{D}_M$, $\psi(\cdot)$ is of class C^1.

For particular x_0, $|\tilde{a}(\cdot)|$ is monotonic along $\psi(\bar{u}, x_0, t)$, from x_0 to $(0, 0)^T$, and hence achieves its maximum at x_0. One can easily obtain that, the region $\mathcal{Q}$ of such initial conditions contains $\mathcal{D}_M$ and is bounded as follows: if $(cx_M)(cb) > 0$, by lines $cA(x - x_M) = 0$, $cAx = 0$, and the two trajectories with $u = M$ passing resp. through $(0, 0)^T$ and x_σ, with x_σ s.t. $cA(x_\sigma - x_M) = 0$ and $cx_\sigma = 0$; otherwise, if $(cx_M)(cb) \leq 0$, by lines $cA(x - x_M) = 0$, $v^Tx = 0$, and the trajectory with $u = M$ passing through $(0, 0)^T$.

If $x_0 \notin \mathcal{Q}$, $|\tilde{a}(\cdot)|$ achieves a maximum along $\psi(\bar{u}, x_0, t)$, for some time $\tau > 0$ such that $x_\tau = \psi(\bar{u}, x_0, \tau)$ satisfy either $cA(x_\tau - x_M) = 0$ or $cAx_\tau = 0$. Optimality of control (13) is proved by showing that at time τ, any other control $u \in \mathcal{U}$, different from $\bar{u}$, achieves a value of $|\tilde{a}(\cdot)|$ which cannot be lower than $|c\psi(\bar{u}, x_0, \tau)|$:

$$|c\psi(\bar{u}, x_0, \tau)| \;\leq\; |c\psi(u, x_0, \tau)| \;\leq\; \sup_{0 \leq t \leq T} |c\psi(u, x_0, t)| \text{ for any } u \neq \bar{u} \in \mathcal{U}\;. \tag{16}$$

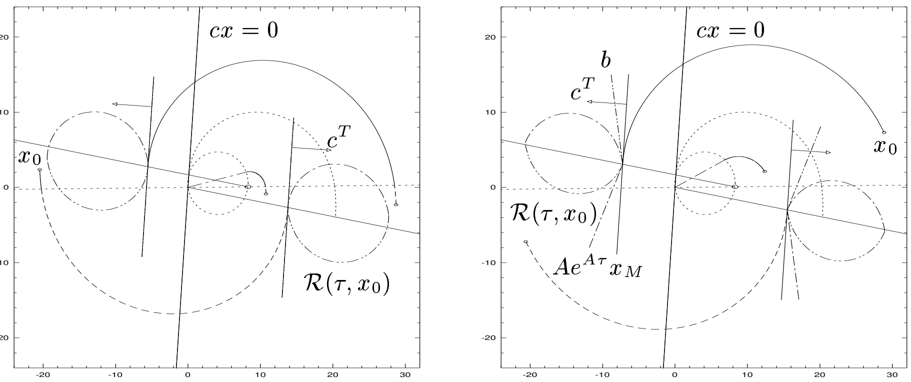

Case (a) Case (b)

Fig. 3. Reachable sets for final conditions on the locus of points maximum.

Such inequality will be proved analyzing the reachable set $\mathcal{R}(\tau, x_0)$. From Proposition 8, we have $\tau \leq \frac{\pi}{\mu}$. Consider $x_0 \notin \mathcal{D}_M$. Two cases are in order either: (a) $\bar{u}(t)$ has a discontinuity point for some $\bar{\tau} \in [0, \tau]$, or (b) $\bar{u}(t)$ is constant in $[0, \tau]$.

(a) We first show that, in this case, $\frac{dx}{dt}(\tau)$ is collinear to the line s passing through x_τ and parallel to $Ae^{A(\tau-\bar{\tau})}x_M$. Consider $\bar{u}(t) = 0$ for $t \in [0, \bar{\tau})$ and $\bar{u}(t) = M$ for $t \in [\bar{\tau}, \tau]$. We have $\frac{dx}{dt}(\tau) = Ae^{A\tau}\left(x_0 - e^{-A\bar{\tau}}x_M\right)$. But, since from (13) the operator $e^{A\bar{\tau}}$ steers point x_0 to the swicthing line $v^T x = 0$, $e^{-A\bar{\tau}}$ maps x_M (which lies on $v^T x = 0$) to a vector collinear to x_0. Then, $\frac{dx}{dt}(\tau)$ is parallel to $Ae^{A(\tau-\bar{\tau})}x_M$. If, instead, $\bar{u}(t) = M$ for $t \in [0, \bar{\tau})$ and $\bar{u}(t) = 0$ for $t \in [\bar{\tau}, \tau]$, $\frac{dx}{dt}(\tau) = Ae^{A\tau}\left((x_0 - x_M) + e^{-A\bar{\tau}}x_M\right)$ and, analogously to above, $e^{-A\bar{\tau}}$ maps x_M to a vector collinear to $x_0 - x_M$. Hence, in both cases $\frac{dx}{dt}(\tau)$ is collinear to s. Furthermore, from (15) one can easily obtain that line s is also tangent to $\partial\mathcal{R}(\tau, x_0)$ at x_τ. Due to the convexity property of the reachable set, $\mathcal{R}(\tau, x_0)/x_\tau$ is all located on the same side of s, namely the one which does not contain the origin. Since these arguments are valid for any final time, it follows that $\mathcal{R}(t', x_0)$, with $t' \leq \frac{\pi}{\mu}$, is always tangent to $\psi(\bar{u}, x_0, t)$ at $t = t'$.

Now, since by construction, $|\tilde{a}(\cdot)|$ is maximal along $\psi(\bar{u}, x_0, t)$ at $t = \tau$, c is perpendicular to $Ae^{A(\tau-\bar{\tau})}x_M$ and s can be written as $(cx_\tau)\, c(x - x_\tau) = 0$. Since $\forall x \in \mathcal{R}(\tau, x_0)/x_\tau$, $(cx_\tau)\, c(x - x_\tau) > 0$, condition (16) holds for any $u \neq \bar{u}$.

(b) If instead $\bar{u}(t)$ is constant in $[0, \tau]$, necessarily, x_τ equals either $x^{(0)}$ or $x^{(M)}$ and, hence, $\partial\mathcal{R}(\tau, x_0)$ is not of class C^1 at x_τ. Evaluating from (15) the tangent vectors to $\gamma_0(\cdot)$ or $\gamma_M(\cdot)$ at x_τ, one obtains a direction parallel to b (with $\alpha = \tau$) and a direction parallel to $Ae^{A\tau}x_M$ (with $\alpha = 0$). Further, it is easy to check that, for the same x_τ, the latter ranges from the line parallel to b (as $x_0 \to x_\tau$) and the line perpendicular to c^T (as $v^T x_0 \to 0$). Vector b is not collinear to $\frac{dx}{dt}(\tau)$ expect for x_τ lying on $v^T x = 0$. Then, also in this case, we can conclude that $\mathcal{R}(\tau, x_0)/x_\tau$ on the side of $c(x - x_\tau) = 0$ opposite to the origin, and $\forall x \in \mathcal{R}(\tau, x_0)/x_\tau$, $(cx_\tau)\, c(x - x_\tau) > 0$. Hence, (16) holds.

Moreover, suppose now that $\psi(\bar{u}, x_0, t)$ enters $\mathcal{D}_M$ with $\bar{u} = 0$, through $v^T x = 0$. Consider $\tau = \min\{t | (v^T \psi(0, x_0, \tau) = 0\}$. The boundary of the set of points reachable in time $t \leq \tau$ is given by curves $\gamma_M(\alpha)$, $e^{A\alpha}x_0 + (I - e^{A\alpha})x_M$ and $e^{A\alpha}x_0 = \psi(0, x_0, \alpha)$ with $\alpha \in [0, \tau]$. Hence, any other control, which steers x_0 to the origin, cannot achieve a value of the cost function smaller than $|cx_\tau|$, since curve $\psi(0, x_0, \alpha)$ with $\alpha \in [0, \tau]$ can never be crossed for it is a piece of the boundary of the reachable set.

Control (13) is not an optimal solution to Problem 2 for, as discussed in [1], it does not provide finite time convergence to B_ρ for $x_0 \in \mathcal{D}_M$ s.t. $v^T x_0 = 0$. Rotating switching line $v^T x = 0$ by a $\theta > 0$, convergence to B_ρ within a finite time is achieved.

If $(cx_M)(cb) > 0$, $\bar{u}$ as in (13), with $\theta \in (0, \cos^{-1}(|b^T v|\, \|b\|^{-1})$, is again an optimal solution to Problem 2. In fact, since the center of $\mathcal{C}_M$ belongs to $(R(\theta)v)^T x = 0$ with $\theta = \cos^{-1}(|b^T v|\, \|b\|^{-1}))$ and $\psi(0, x_0, t)$ is convergent to the origin, for any θ in the interval above $x(t) = \psi(0, x_0, t)$, with $x_0 \in \mathcal{D}_M$ s.t. $(R(\theta)v)^T x_0 > 0$, reaches line $(R(\theta)v)^T x = 0$ in a point contained in $\mathcal{D}_M$. For $(cx_M)(cb) > 0$, $|\tilde{a}(\cdot)|$ monotonically decreases along $\psi(0, x_0, t)$ and hence $\bar{u}$ is optimal. Conversely, if $(cx_M)(cb) \leq 0$, for any $x_0 \in \mathcal{D}_M$ between lines $cAx = 0$ and $v^T x = 0$, $|\tilde{a}(\cdot)|$ monotonically increases along $\psi(0, x_0, t)$. Let $\theta_{cA} = \cos^{-1}(|cAv|\, \|cA\|^{-1})$ denote the angle between lines $cAx = 0$ and $v^T x = 0$. For any $\theta \in (0, \theta_{cA})$, given $x_0 \in \mathcal{D}_M$ s.t. $v^T x_0 = 0$, $|\tilde{a}(\cdot)|$ is maximum at $\psi(0, x_0, \theta/\mu)$ on line $(R(\theta)v)^T x = 0$, and

$$\lim_{\theta \to 0^+} \{ \max_{t \in [0,T]} |c\psi(0, x_0, t)| \} = \lim_{\theta \to 0^+} |c\psi(0, x_0, \theta/\mu)| = |cx_0|.$$

Hence, given any $\theta_1 \in (0, \theta_{cA})$, one can always find $\theta \in (0, \theta_{cA})$ such that $|c\psi(0, x_0, \theta/\mu)| < |c\psi(0, x_0, \theta_1/\mu)|$. For any $x_0 \in \mathcal{D}_M$ which can be steered to $(R(\theta)v)^T x = 0$ with $u = 0$, an upper bound for $|c\psi(0, x_0, \theta/\mu)| - |cx_0|$ is given by $|c\left(e^{-A\frac{\theta}{\mu}} - I\right) v_\perp| \frac{M}{\mu} \|b\|$. Hence, for any $\epsilon > 0$, choosing $\theta \in (0, \theta_{cA})$ if $|c\left(e^{-A\frac{\theta_{cA}}{\mu}} - I\right) v_\perp| \frac{M}{\mu} \|b\| < \epsilon$, or $\theta \in (0, \theta_c)$ with θ_c solution to equation $|c\left(e^{-A\frac{\theta_c}{\mu}} - I\right) v_\perp| \frac{M}{\mu} \|b\| = \epsilon$, yields $\sup_{0 \leq t \leq T} |c\psi(\bar{u}, x_0, t)| - \tilde{A} < \epsilon$. Q.E.D.

4 Hybrid system control scheme

Control law (13) is clearly not feasible for the hybrid model $\mathcal{M}_{4cyl}$, introduced in Section 2, for three main reasons:

- (a) available torque is limited to 0 and to interval $[r_{min}M, M]$;
- (b) there is a delay between the time of injection and the time at which the corresponding torque is generated;
- (c) torque generation has to be synchronized with the powertrain dynamics.

Our solution to point (a) is to use bang–bang control everywhere in the state space, introducing an appropriate switching surface $\sigma(x) = 0$. To simplify discussion of point (b), set $x(k) := x(t_k)$ and $u(k) := u(t_k)$ for all k. Control signal $j_i(k)$, at current time t_k corresponding to an $E \to H$ transition of the $i-$th cylinder, will produce, at the next expansion run of the $i-$th cylinder, the torque $u(k+3)$. Such signal will feed the continuous system during the interval $[t_{k+3}, t_{k+4})$, steering the state from $x(k+3)$ to $x(k+4)$. A prediction of $x(k+3)$ is obtained from $x(k)$ by a forward integration of (5). Because of the synchronization constraint mentioned in (c), switchings of the torque u cannot occur, in general, exactly on $\sigma(x) = 0$. This issue is the main difficulty for devising a robust control strategy and is the main subject of this section.

If it is predicted that $x(t)$ will cross the switching surface $\sigma(x) = 0$ at some $t \in (t_{k+3}, t_{k+4})$, one can decide to switch j_i either at t_k or t_{k+1}. In certain conditions if switching is anticipated, an acceleration peak may be introduced. For this reason, we decide to switch always at time t_{k+1}, i.e.

$$\hat{j}_i(k) = \begin{cases} 0 & \text{if } x(k+3) \in B_\rho \\ \begin{cases} 0 \text{ if } \sigma(x(k+3)) \geq 0 \\ 1 \text{ if } \sigma(x(k+3)) < 0 \end{cases} & \text{if } x(k+3) \notin B_\rho \,. \end{cases} \tag{17}$$

Control law (17) may fail to switch injection to 0 when state x enters B_ρ, and possibly go into a limit cycle. If $u(t) = M$, for $t \in [t_{k+3}, t_{k+4}]$, there may be crankshaft speeds such that delay $t_{k+4} - t_{k+3}$ causes the trajectory $\psi(M, x(t_{k+3}), t)$ to intersect B_ρ leaving both decision points $x(k+3)$ and $x(k+4)$ outside B_ρ. A necessary condition for this not to happen is to have $\|x(t_{k+4})\| < \|x(t_{k+3})\|$. The locus of points which under control $u = M$ increase their norm in time Δ is

$$\mathcal{N}_\Delta = \{x \mid \|x\| < \|e^{A\Delta}(x - x_M) + x_M\|\}\,. \tag{18}$$

Suppose there exist two distinct intersections of the boundaries of B_ρ and $\mathcal{N}_\Delta$, namely $x_c^{(1)}$ and $x_c^{(2)}$, as shown in Figure 4. Let $\psi_{M^-}(x, \alpha) = e^{-A\frac{\alpha}{\mu}}(x - x_M) + x_M$ be the point such that $\psi(M, \psi_{M^-}(x, \alpha), \frac{\alpha}{\mu}) = x$. Let $\psi_c^{(1)}(\cdot)$ and $\psi_c^{(2)}(\cdot)$ be the curves $\psi_c^{(1)}(\alpha) = \psi_{M^-}(x_A, \alpha)$, and $\psi_c^{(2)}(\alpha) = \psi_{M^-}(x_B, \alpha)$, with $\alpha \in [-\frac{\pi}{2}, \pi]$, where x_A, x_B are such that $v^T x_A = 0$, $v^T x_B = 0$, $v_\perp^T(x_A - x_M) < 0$, $v_\perp^T(x_B - x_M) < 0$ and $x_c^{(1)} \in \psi_c^{(1)}(\cdot)$, $x_c^{(2)} \in \psi_c^{(2)}(\cdot)$. Let $x_D = \psi_c^{(2)}(\pi)$, and define the switching function in (17) as

$$\sigma(x) = \begin{cases} (v^T b/\|b\|)^{-1} v^T x & \text{if } ({b_\perp}^T x \leq {b_\perp}^T x_B) \;\vee\; ({b_\perp}^T x \geq {b_\perp}^T x_D) \\ & \\ (b/\|b\|)^T (x - x') & \text{if } {b_\perp}^T x_B < {b_\perp}^T x < {b_\perp}^T x_D \\ \text{with } x' \text{ s.t. } ({b_\perp}^T (x - x') = 0) \;\wedge (\; x' \in \psi_c^{(2)}) & \end{cases} \tag{19}$$

Control $\hat{j}_i(k)$ in (17) switches on the curve described as follows (see Figure 4): the half line $v^T x = 0$ with $v_\perp^T(x - x_\rho) \leq 0$, and $x_\rho = -\rho v_\perp$; the arc of the boundary of B_ρ from x_ρ to $x_c^{(2)}$; the arc of $\psi_c^{(2)}(\cdot)$ from $x_c^{(2)}$ to x_D; the half line $v^T x = 0$ with $v_\perp^T(x - x_D) \geq 0$. Such choice can prevent from the existence of limit cycles as illustrated in the following lemma.

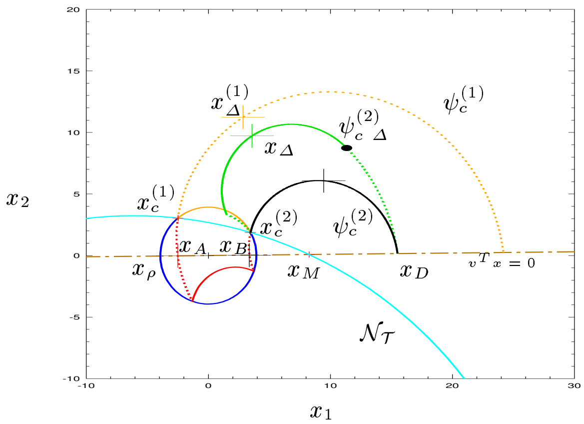

Fig. 4. Derivation of the hybrid switching surface.

Lemma 10. *If $\|x_M\| > \rho$, there exists a ω_{cmin} finite such that, substituting Δ in (18) for $\Delta_{max} = \frac{30}{\omega_{cmin}}$ (with ω_{cmin} in rpm), if a trajectory of system $\mathcal{M}_{4cyl}$ under control law $\hat{j}_i(k)$ as in (17), with $\omega_c(t) \geq \omega_{cmin} = \forall t \geq 0$, intersects $\sigma(x) = 0$ trough the arc $\psi_c^{(2)}(\alpha)$ with $\alpha \in [0, \pi]$ at some time $\bar{t} \in [t_{k+3}, t_{k+4}]$, then $x(t) \in B_\rho$ for all $t > t_{k+4} + \frac{3\pi}{2\mu}$.*

Proof. Note that $\lim_{\Delta \to 0} \mathcal{N}_\Delta = \mathcal{N}_0$, where $\mathcal{N}_0$ is the disk with boundary passing by both x_M and the origin 0 and center in $-\frac{M}{2\lambda} b$. From hypothesis $\mid x_M \mid > \rho$

$$\exists x_c^{(1)},\ x_c^{(2)}\ \in \mathbb{R}^2,\ \text{with } x_c^{(1)} \neq x_c^{(2)}. \tag{20}$$

By continuity and monotonicity, there exists a finite time $\Delta_{max1} > 0$ and correspondingly a speed $\omega_{cmin1} = \frac{30}{\Delta_{max1}}$, such that for all $\Delta < \Delta_{max1}$, (20) holds and (19) is well–defined.

Under the hypotheses of the Lemma, all points $x(k+4)$ belong to the set

$$\mathcal{S}_\Delta = \left\{ x : x = e^{A\delta} \psi_c^{(2)}(\alpha), \text{with } \ \alpha \in [0, \pi] \ \text{ and } \delta \in [0, \Delta] \right\}, \tag{21}$$

with boundaries: $\psi_c^{(2)}(\alpha)$ with $\alpha \in [0, \pi]$; $\psi_{c\Delta}^{(2)}(\cdot)$, where $\psi_{c\Delta}^{(2)}(\alpha) = e^{A\Delta} \psi_c^{(2)}(\alpha)$, with $\alpha \in [0, \pi]$; $\psi(0, x_D, \delta)$, with $\delta \in [0, \Delta]$; $\psi(0, x_B, \delta)$, with $\delta \in [0, \Delta]$.

If $x(k+4) \in B_\rho$, $\hat{j}_i(k+1) = 0$ and $x(t) \in B_\rho$ $\forall t \geq t_{k+4}$. If $x(k+4) \notin B_\rho$, $\hat{j}_i(k+1) = 1$. If $\mathcal{S}_\Delta \cap \psi_c^{(1)}(\cdot) = \emptyset$, then the trajectory $\psi(M, x(k+4), t)$ originating at $x(k+4)$ under $u(t) = M$ enters B_ρ through the arc from $x_c^{(1)}$ to $x_c^{(2)}$. Since $\mid x_M \mid > \rho$, $\psi(M, x(k+4), t)$ reaches B_ρ at time $t_\rho \leq t_{k+4} + \frac{3\pi}{2\mu}$.

By construction there exists a $\bar{K} > k+4$ such that $x(\bar{K}-1) \notin B_\rho$ and $x(\bar{K}) \in B_\rho$, since $x(\bar{K}-1) \notin \mathcal{N}_\Delta$, with $t_{\bar{K}-1} < t_\rho \leq t_{\bar{K}}$. Consequently injection switches to zero, and $x(t) \in B_\rho$, $\forall t \geq t_\rho$. $\lim_{\Delta \to 0} \psi_{c\ \Delta}^{(2)}(\cdot) = \lim_{\Delta \to 0} \mathcal{S}_\Delta = \psi_c^{(2)}(\cdot)$

Necessarily $\mathcal{S}_\Delta \cap \psi_c^{(1)}(\cdot) = \emptyset$. By continuity and monotonicity, there exists a finite time $\Delta_{max} > 0$ with $\Delta_{max} < \Delta_{max1}$ and correspondingly a speed $\omega_{cmin} = \frac{30}{\Delta_{max}}$ such that for all $\Delta < \Delta_{max}$ $\mathcal{S}_\Delta \cap \psi_c^{(1)}(\cdot) = \emptyset$. Q.E.D.

To find Δ_{max} of Lemma 10, we derive a function $f(\Delta)$ which is positive if $\mathcal{S}_\Delta \cap \psi_c^{(1)} = \emptyset$, negative otherwise. We first determine the trajectory $\psi_c^{(\Delta)}$, where $\psi_c^{(\Delta)}(\alpha) = \psi_{M^-}(\bar{x}_\Delta, \alpha)$, with $\alpha \in [0, \pi]$, and $v^T \bar{x}_\Delta = 0$ such that $\psi_c^{(\Delta)}$ is tangent to $\psi_{c\Delta}^{(2)}$ at point $x_\Delta = \psi_{c\Delta}^{(2)}(\alpha_\Delta)$. At point x_Δ

$$-\left.\frac{\partial \psi_{c\Delta}^{(2)}(\alpha)}{\partial \alpha}\right|_{\alpha=\alpha_\Delta} // A\left(\psi_{c\Delta}^{(2)}(\alpha_\Delta) - x_M\right). \tag{22}$$

Condition (22) is satisfied for $\alpha_\Delta = \mu\Delta + \cos^{-1}\ v_\perp^T\ \overrightarrow{vers}\ (e^{A\Delta}x_M - x_M)$. Consider $x_\Delta^{(1)} = \psi_c^{(1)}(\alpha_\Delta^{(1)})$, with $\alpha_\Delta^{(1)} = \cos^{-1}\ v_\perp^T\ \overrightarrow{vers}\ (x_\Delta)$, and define $f(\Delta) = \|x_\Delta^{(1)} - x_M\| - \|x_\Delta - x_M\|$. Control $\hat{\jmath}_i$ does not lead to limit cycles when crossing $\psi_{c\Delta}^{(2)}$ if

$$f(\Delta) = \|x_\Delta^{(1)} - x_M\| - \|x_\Delta - x_M\| > 0. \tag{23}$$

Convergence of the trajectories intersecting the switching surface on $\psi_c^{(2)}$ is addressed in the previous lemma. However, we need to prove convergence for all initial conditions.

Let us compare the trajectories when intersecting the line $v^T x = 0$, which is the optimal switching surface for the continuous case. In the hybrid case, the switching occurs with some delay due to the discretization of the decision points. There are two cases to analyze: **a**) $v_\perp^T x < 0$, i.e. the intersection is to the left of B_ρ, **b**) $v_\perp^T (x - x_M) > 0$, i.e.the intersection is to the right of B_ρ.

In both cases, we can bound the difference between the value of the norm of the points on the optimal trajectory and those corresponding to the hybrid control law. We can also compare the performance of the hybrid control law with respect to accelerations peaks. Note that since the switchings occur at different points, we compare the points on the next intersection on the optimal switching line $v^T x = 0$, to be able to compare norms.

Let x_{M0} be such that $v^T x_{M0} = 0$, with $v_\perp^T x_{M0} < 0$. Consider the point $x_{M0}^{(2)}$ reached under control $u = M$ for Δ seconds, i.e., the point that corresponds to the switching of control occurring as far as possible from the optimal switching surface. The hybrid trajectory then reaches $v^T x = 0$ at point $x_{M0}^{(3)}$ under control $u = 0$, that is

$$x_{M0}^{(2)} = e^{A\,\Delta}(x - x_M) + x_M, \quad x_{M0}^{(3)} = \left(e^{A\frac{1}{\mu}\cos^{-1} v_\perp^T \overrightarrow{vers}(x_{M0}^{(2)})}\right) x_{M0}^{(2)}.$$

Let $x_{M0}^{(1)} = e^{A\frac{\pi}{\mu}} x_{M0}$ be the point reached by the continuous trajectory from x_{M0}, we define

$$w^0(x_{M0}, \Delta) = \|x_{M0}^{(3)}\| - \|x_{M0}^{(1)}\|, \quad w_a^0(x_{M0}, \Delta) = |cy_\perp| e^{-\frac{\lambda}{\mu}\alpha_c} w^0(x_{M0}, \Delta),$$

the increase in norm due to non optimal switching and the corresponding increase in the peak following the transition, where $\alpha_c = \cos^{-1}(v^T y)$.

Let x_{0M} be such that $v^T x_{0M} = 0$ and $v_\perp^T(x_{0M} - x_M) > 0$, and analogously to the previous case, consider the points $x_{0M}^{(1)} = \psi(M, x_{0M}, \frac{\pi}{\mu})$ and $x_{0M}^{(2)} = \psi(0, x_{0M}, \Delta)$ respectively on the continuous and on the hybrid trajectory, the latter subsequently reaches $x_{0M}^{(3)} = \psi(M, x_{0M}^{(2)}, \frac{1}{\mu}\cos^{-1}\frac{v_\perp^T x_{0M}^{(2)}}{\|x_{0M}^{(2)}\|})$, and with the same meaning we define

$$w^M(x_{0M}, \Delta) = \|x_{0M}^{(3)}\| - \|x_{0M}^{(1)}\|, \quad w_a^M(x_{0M}, \Delta) = |cy_\perp| e^{-\frac{\lambda}{\mu}\alpha_c} w^M(x_{0M}, \Delta).$$

The two functions $w^0(x_{M0}, \Delta)$ and $w^M(x_{0M}, \Delta)$ bound the increase in norm due to the late switching for the $u = M \to u = 0$ transition and for the $u = 0 \to u = M$ transition of torque value respectively. Not surprisingly, both functions are monotonically decreasing with respect to $\|x_{M0}\|$,$\|x_{0M}\|$ and $\omega_c = \frac{30}{\Delta}$, that is the increase in norm is less for high revolution speeds and for initial conditions that are far from B_ρ.

Now we are ready to discuss the convergence of the control law. Here we have to show that the trajectories originating from points away from B_ρ tend towards B_ρ. To do so, we show that the norm of two consecutive intersection points of the same trajectory under the hybrid control law on $v^T x = 0$, $v_\perp^T(x - x_D) \geq 0$ decreases. Because of the monotonic behavior of $w^0(x_{M0}, \Delta)$ and $w^M(x_{0M}, \Delta)$, the worst initial condition is the closest to the origin which may not switch between $\psi_c^{(1)}$ and $\psi_c^{(2)}$. To identify such initial condition, consider figure 5.

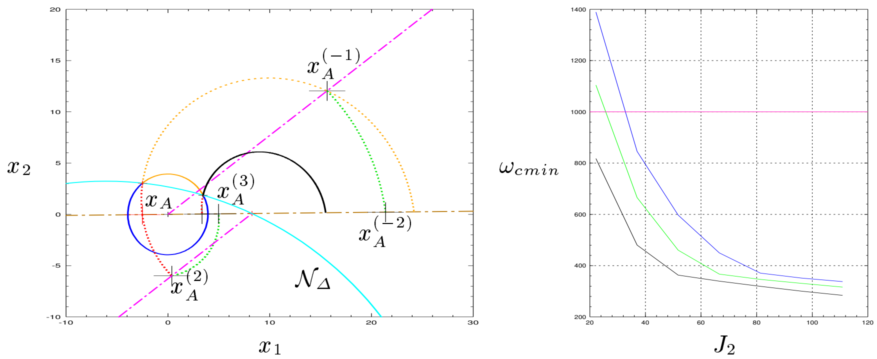

Fig. 5. Limiting trajectory and Parameters ranges.

The trajectory obtained by back integration from x_A with torque $u = M$ switches to $u = 0$ at some point x_s between $v^T x = 0$ and $\hat{v}^T x = 0$, where $\hat{v} = e^{-\lambda\Delta} e^{A\Delta} v$. The worst point is $x_s = x_A^{(-1)} = \psi_c^{(1)}(\alpha_\Delta^{(-1)})$, with $\alpha_\Delta^{(-1)} \in [0, \pi]$

solution to $\hat{v}^T\psi_c^{(1)}(\alpha)=0$. In fact points on $\hat{v}^T x=0$ correspond to a switching occurring with the maximum delay Δ with respect to the ideal switching. Now, let $x_A^{(-2)}=e^{-A\Delta}x_A^{(-1)}$ be the point on $v^T x=0$ from which the latest switching from $u=0$ to $u=M$ leads to x_A. All other points on $v^T x=0$ with $0<v_\perp^T x<v_\perp^T x_A^{(-2)})$ fall into B_ρ and are characterized by Lemma 10. Let $x_A^{(3)}$ be the point on $v^T x=0$ after a late switching from x_A, then $\|x_A^{(-2)}\|-\|x_A^{(3)}\|$ bounds from below the decrease in norm on the trajectory between two consecutive intersection points with $v^T x=0$, $v_\perp^T(x-x_A^{(-2)})\geq 0$, due to the way we picked the switching surfaces and x_A. If indeed

$$\|x_A^{(-2)}\|-\|x_A^{(3)}\| \;=\; \|x_A^{(-1)}\|e^{-\lambda\Delta} \;-\; \|x_A\|e^{\frac{\lambda}{\mu}\pi}-w^0(x_A,\Delta)\;>\;0 \tag{24}$$

then, all the other initial conditions farther than $x_A^{(-2)}$ from the origin yield trajectories with decreasing norms, and the control law is convergent.

In the end, control law $\hat{j}_i$ is convergent for all $\omega_c\geq\frac{30}{\Delta}$, if Δ is such that

C1 $\partial\mathcal{N}_\Delta\;\wedge\;\partial B_\rho\;\neq\;\emptyset$, i.e. if $\exists\; x_c^{(1)},x_c^{(2)}\in\mathbb{R}^2$ so to construct $\sigma(x)$ as in (19),
C2 limit cycle condition (23) holds,
C3 norm convergence condition (24) holds.

Performance of the hybrid control law with respect to acceleration peaks can be compared to the continuous one.

Proposition 11. *For any choiche of the parameters, such that conditions* **C1**, **C2**, **C3** *are satisfied, and $(cx_M)(cb)>0$, there exists a $\rho_A>0$ such that:*

Given x_0 with $\|x_0\|>\rho_A e^{-\frac{\pi\lambda}{\mu}}$, let $\bar{x}=\psi(\bar{u},x_0,\bar{t})$, with $\bar{t}\in[0,T]$ and $\bar{u}$ as in (13), be such that $\max_{t\in[0,T]}|c\psi(\bar{u}(x),x_0,t)|\;=\;|c\bar{x}|$. Let $\hat{T}$ be such that $\psi(\hat{u},x_0,\hat{T})\in\partial B_\rho$, with $\hat{u}$ given by $\mathcal{M}_{4cyl}$ under control $\hat{j}_i(k)$. Let $\hat{x}=\psi(\hat{u},x_0,\hat{t})$, with $\hat{t}\in[0,\hat{T}]$, be such that $\max_{t\in[0,\hat{T}]}|c\psi(\hat{u},x_0,t)|\;=\;|c\hat{x}|$, and let $x^v=\psi(\hat{u},x_0,t^v)$, with $t^v\in[0,\pi/\mu]$ be such that $v^T x^v=0$. Then, if $v^T x_0<0$

$$0\leq|c\hat{x}|-|c\bar{x}|\leq w_a^0(x^v,\Delta_{max})\leq w_a^0(-\rho_A v_\perp,\Delta_{max}), \tag{25}$$

where $\Delta_{max}=\frac{30}{\omega_{cmin}}$. If $v^T x_0\geq 0$

$$0\leq|c\hat{x}|-|c\bar{x}|\leq w_a^M(x^v,\Delta_{max})\leq w_a^M(\rho_A v_\perp,\Delta_{max}). \tag{26}$$

In particular $\hat{j}_i(k)$ is optimal for Problem 1, i.e. $|c\hat{x}|-|c\bar{x}|=0$ if x_0 belongs to either $\mathcal{R}_3=\{x\mid v^T x<0,\;y^T(x-x_M)<0\}$ or $\mathcal{R}_4=\{x\mid v^T x>0,\;y^T x>0\}$.

5 Experimental Results

The proposed cut–off control strategy has been implemented and tested at Magneti-Marelli Engine Control Division on a commercial car, a 16 valve 1400 cc engine car equipped with drive-by-wire electronics. The engine control electronics is a 4LV Magneti Marelli on board computer based on a 25MHz 32–bit

Althair Motorola microprocessor with fixed point arithmetic unit. The experiment was carried out driving the car in the test ring and measuring the important parameters and variables that determine the performance of the control strategy.

5.1 Model Parameters

The continuous powertrain dynamics of the car is described by

$$A^p = \begin{bmatrix} 0 & 1 & -7.556 \\ -448.1 & -5.186 & 30.87 \\ 3.042 & .02773 & -.2105 \end{bmatrix}, \quad b^p = \begin{bmatrix} 0 \\ 15.05 \\ 0 \end{bmatrix},$$

and have dominant pole $\lambda_1 = -0.05460$ and complex poles $\lambda \pm j\mu = -2.671 \pm j21.54$, where the parameters of the model were carefully identified on the actual engine. The output map from states $\zeta = [\alpha_e, \omega_c, \omega_p]^T$ to the vehicle acceleration a (in meters per square second) is $c^p = [.8022,\ .007313,\ -.05525]$. The maximum torque achievable when the engine is idle with spark advance $r = 1$, is $M = 12.41$ Nm. The state space transformation matrix

$$P = \begin{bmatrix} 0.05155 & 0.04924 & 7.252 \\ 20.83 & 0.12780 & -0.5979 \\ 0.1596 & -0.9517 & 7.195 \end{bmatrix}$$

allows us to rewrite the powertrain dynamics in the uncoupled form (4) :

$$\begin{bmatrix} b' \\ b \end{bmatrix} = \begin{bmatrix} .7410 \\ 1.923 \\ -14.32 \end{bmatrix}, \quad [c',\ c] = [-1.857\,10^{-3},\ 3.726\,10^{-2},\ -2.523\,10^{-3}]\ .$$

The acceleration perception threshold was set to 0.03 the acceleration due to gravity. Hence ρ is 7.872.

5.2 Convergence Analysis

Before starting the experimentation of the proposed control algorithm, a corner analysis with respect to the vehicle inertia momentum J_2 was carried out, in order to establish the minimum crankshaft speed ω_{cmin} for which (17) converges. Figure 5 reports the minimum crankshaft speed, obtained from conditions **C1**, **C2**, **C3**, for a given J_2 and for spark advance modulation factor r_i in $\{0.6, 0.8, 1\}$. It is interesting to note that, acting on the spark advance, one can reduce substantially ω_{cmin}. For the identified value $J_2 = 73.95$, we have $\omega_{cmin} \simeq 396rpm$, $356rpm$, $329rpm$, respectively for $r_i = 1$, 0.8, 0.6.

To prevent engine from stopping, cut-off strategies are usually not applied for $\omega_c <\simeq 1000rpm$. With the identified parameters, for $\omega_c = 1000rpm$, $f(\Delta) \simeq 8.22$, $\|x_A^{(-2)}\| - \|x_A^{(3)}\| \simeq 7.92$, hence convergence of (17) is ensured.

5.3 Discussion

The cut-off control strategy is applied after the accelerator pedal is released and the manifold pressure is equal to 300 mbar. A simple Leunberger observer is used to estimate the state of the powertrain's continuous dynamics, from which the oscillatory components $\hat{x}$ are derivered. The initialization procedure computes also the observer gain matrix L, to obtain satisfactory convergence of the observer. The switching function $\sigma(x)$, given in section 4, has been described by piecewise linear approximation with 20 points.

In the sequel the performances achieved by the proposed cut-off strategy are compared with the performance of a currently implemented open-loop strategy and with an instantaneous uncontrolled cut-off operation. Figure 6 shows the evolution of $\hat{x}$ components of observer state during a cut-off operation. The switching curve $\sigma(x) = 0$, as it is approximated in the implementation, is reported along with B_ρ. Next, the evolution of the crankshaft speed, in rpm, is reported next. Only a significant positive peak is recognizable in the crankshaft speed. Such behavior is also shown in the next plot in terms of vehicle acceleration. As expected, once injection is set to zero permanently $\tilde{a}(t)$ remains bounded within the perception threshold. Finally, the last plot shows the evolution of the injection signal.

The experimental results fully confirm the theory of Section 4. When comparing this strategy with the open loop strategy used in the previous implementation, we observed a much better performance in terms of acceleration peaks and driving comfort. One could argue that this improvement, predicted by the theory, has been obtained with a more expensive implementation. Actually our strategy resulted in a much smaller memory occupation and in a very reasonable CPU time. In fact, the code size was 70% and the data size was 50% of the ones needed by the previously implemented strategy. The CPU power needed to run the control algorithm was about 1% of the available computing power. In addition, our strategy, being closed loop, needed much less tuning effort than the open loop strategy.

6 Conclusions and future work

In this paper, we presented a novel approach to engine control in the cut-off region, based on a hybrid model of the torque generation and of the power-train dynamics in a four-stroke engine. A control problem on this hybrid system is defined and solved using a sequence of approximations. The properties of the control law so obtained have been characterized, thus offering better confidence on the quality of the results with respect to commonly used heuristic, open loop, approaches. In addition, since the control law is closed loop, expensive tuning processes can be avoided yielding a commercially appealing solution. We expect to see the final version of the control laws in products by the first half of 1998. In addition, we expect to extend the approach to the problem of idle speed control that shares several key features with the cut-off control problem.

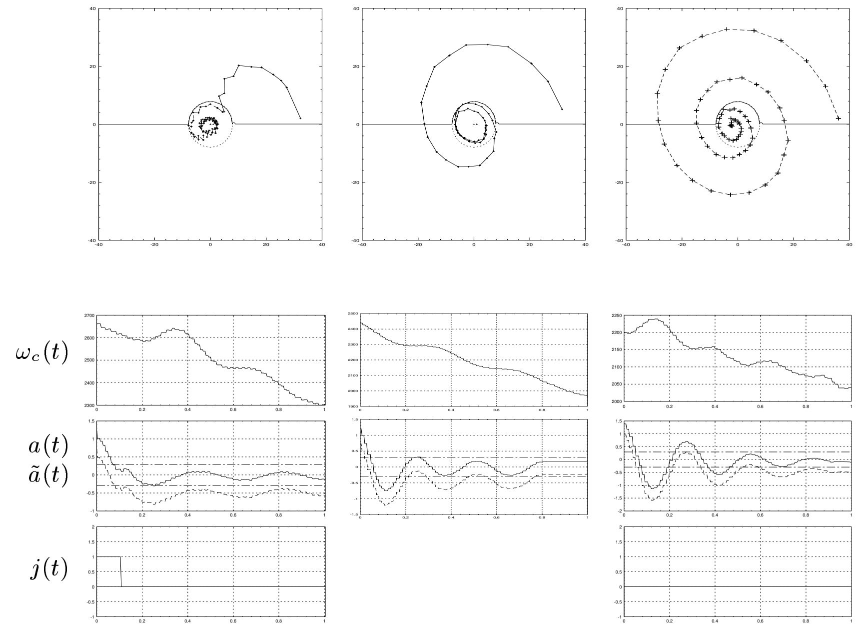

Fig. 6. Evolutions in the $\hat{x}$ sub–space of observer state during cut-off operations. From left to right: the proposed control, a currently implemented strategy and instantaneous cut-off. State samples are linked by a continuous arc if in the previous cycle injection took place, dotted one if it did not. Evolution of the corresponding revolution speed (in rpm), vehicle acceleration (in m^2/second, dotted line represents total acceleration $a(t)$ and continuous line represents the oscillating component $\tilde{a}(t)$), and injection signal.

7 Acknowledgments

This research has been partially sponsored by PARADES, a Cadence, Magneti-Marelli and SGS-Thomson GEIE, and by CNR. We wish to acknowledge the support of the management of Magneti Marelli, and, in particular of Drs. Pecchini, Mortara and Romeo, without which this work would not have been possible. ISI provided the X-Math environment to carry out the simulation and the development of the control law. Dr. Alberto Ferrari developed two powerful simulation environments, both including X-Math. One is based on Ptolemy, a University of California simulation and design tool for heterogeneous systems, the other on BoNES, a commercial simulation tool from the Alta group of Cadence, These environments have been essential to develop, tune and implement the control strategy. Dr. Luca Benvenuti offered insightful comments on the results of the paper.

References

1. A. Balluchi, M. D. Benedetto, C. Pinello, C. Rossi, and A. Sangiovanni-Vincentelli, *Cut-off in engine control: a hybrid system approach*, in 36th CDC, San Diego, CA, 1997.
2. J. B. Heywood, *Internal Combustion Engine Fundamentals*, McGraw-Hill Book Co., Inc., NY, 1989.
3. C. Horn and P. J. Ramadge, *Robustness issues for hybrid systems*, in 34th CDC., New Orleans, LA, 1995, pp. 1467–1472.
4. L. Hou, A. Michel, and H. Ye, *Stability analysis of switched systems*, in 35th CDC, Kobe, Japan, 1996, pp. 1208–1212.
5. A. S. Morse, ed., *Control using logic–based switching*, vol. 222 of Lecture notes in control and information sciences, Springer–Verlag, London, U.K., 1997.
6. T. Niinomi, B. H. Krogh, and J. E. R. Cury, *Synthesis of supervisory controllers for hybrid systems based on approximating automata*, in 34th CDC., New Orleans, LA, 1995, pp. 1461–1466.
7. S. Pettersson and B. Lennartson, *Stability and robustness for hybrid systems*, in 35th CDC, Kobe, Japan, 1996, pp. 1202–1207.
8. A. Sangiovanni-Vincentelli, *Embedded system design and hybrid systems*, in Control using logic–based switching, A. S. Morse, ed., vol. 222 of Lecture notes in control and information sciences, Springer–Verlag, London, U.K., 1997, pp. 17–38.
9. H. J. Sussmann, *Lie brackets, real analyticity and geometric control*, in Differential Geometric Control Theory, R. W. Brockett, R. S. Millman, and H. J. Sussmann, eds., vol. 27 of Progress in Mathematics, Birkhäuser, Boston Basel Stuttgart, 1983, pp. 1–117.
10. H. Ye, A. N. Michel, and L. Hou, *Stability theory for hybrid dynamical systems*, in 34th CDC., New Orleans, LA, 1995, pp. 2679–2684.

This article was processed using the LaTeX macro package with LLNCS style